International Journal of Thermophysics, Vol. 1, No. 1, 1980

Thermophysical Measurements on Low Carbon 304 Stainless Steel Above 1400 K by a Transient (Subsecond) Technique

A. Cezairliyan[1] and A. P. Miiller[1]

Received September 27, 1979

Simultaneous measurements, by a subsecond duration transient technique, to determine the specific heat capacity, c_p, the electrical resistivity, ρ, and the hemispherical total emittance in the temperature range 1400–1700 K, and the melting point and the radiance temperature at the melting point, of AISI type 304L stainless steel are described. The results are expressed by the relations:

$$c_p = 1127 - 7.265 \times 10^{-1}\, T + 2.884 \times 10^{-4}\, T^2$$

$$\rho = 75.59 + 4.695 \times 10^{-2}\, T - 9.592 \times 10^{-6}\, T^2$$

where c_p is in $\mathrm{J \cdot kg^{-1} \cdot K^{-1}}$, ρ is in $\mu\Omega \cdot \mathrm{cm}$, and T is in K. The value of the hemispherical total emittance is 0.37 in the range 1700–1900 K. The melting point and the radiance temperature (at 653 nm) at the melting point are 1707 and 1590 K, respectively, yielding a value of 0.385 for the normal spectral emittance at the melting point. Estimated inaccuracies of the measured properties are: 3% for the specific heat capacity, 2% for electrical resistivity, 5% for hemispherical total emittance, and 8 K for melting point and radiance temperature at the melting point.

KEY WORDS: dynamic techniques; electrical resistivity; high temperatures; melting point; radiance temperature; specific heat; stainless steel; thermal emittance.

1. INTRODUCTION

Numerous studies have been carried out on the properties of stainless steels; however, nearly all of these measurements were carried out at temperatures

[1]Thermophysics Division, National Bureau of Standards, Washington, D.C. 20234, U.S.A.

0195-928X/80/0300-0083$03.00/0

below about 1400 K. In this paper, we describe the measurement of selected thermophysical properties of AISI (American Iron and Steel Institute) type 304L stainless steel at temperatures above 1400 K by a subsecond pulse heating technique. The measured properties are: specific heat capacity, electrical resistivity, hemispherical total emittance, melting point,[2] and radiance temperature[3] at the melting point. The measurement technique has been used successfully to obtain thermal and radiative properties of a number of refractory metals and alloys [1].

The method is based on rapid resistive self-heating of the specimen from room temperature to its melting point in less than 1 s by the passage of an electrical current pulse through it; and on simultaneously measuring such experimental quantities as the specimen temperature, the current through and voltage across the specimen. The temperature is measured by means of a high-speed photoelectric pyrometer [2]. The current through the specimen is determined by measuring the voltage across a standard resistance in series with the specimen. The voltage across the middle one-third of the specimen is measured between spring-loaded knife edge probes. These quantities are recorded digitally every 0.4 ms with a full-scale resolution of about 1 part in 8000. Details regarding the construction and operation of the measurement system and other pertinent information such as formulation of relations for properties, error analysis, etc., are given in earlier publications [3, 4].

2. MEASUREMENTS

2.1. Specimens

The measurements of specific heat capacity, electrical resistivity, hemispherical total emittance, and melting point were performed on four specimens in the form of tubes. The tubes were fabricated from rods by removing the center portion by means of an electro-erosion technique. The dimensions of the tubes were, nominally: length, 76 mm; outside diameter, 6.4 mm; and wall thickness, 0.5 mm. A small rectangular sighting hole (0.5×1 mm) was fabricated through the wall at the middle of each tube, thereby approximating a blackbody cavity for the pyrometric temperature measurements. The outer surfaces of the specimens were polished to reduce heat loss due to the thermal radiation.

The radiance temperature measurements at the melting point were

[2]Alloys have a melting range instead of a melting point. For convenience, in the present work the solidus point of the alloy is referred to as the melting point.

[3]Radiance temperature (sometimes referred to as brightness temperature) of the specimen surface is the temperature at which a blackbody has the same radiance as the surface, corresponding to the effective wavelength of the measuring pyrometer.

Table I. Chemical Composition of the Low Carbon 304 Stainless Steel in Percent by Mass

Material form	Elements											
	Fe	Cr	Ni	Mn	C	Si	S	Cu	Co	P	Mo	N
Rod	Major	18.50	9.30	1.16	0.022	0.70	0.011			0.010		0.010
Sheet	Major	18.48	9.38	1.72	0.019	0.60	0.009	0.10	0.18	0.033	0.15	

performed on specimens in the form of strips fabricated from a sheet of the specimen material. The nominal dimensions of the strips were: length, 76 mm; width, 6.4 mm; and thickness, 0.25 mm. The rod and sheet forms of 304 stainless steel were supplied by different manufacturers. Their chemical analyses (of typical material) show little difference in composition, as can be seen in Table I.

2.2. Procedure

All experiments were performed with the specimen in an argon environment at slightly above atmospheric pressure. To optimize the operation of the high-speed pyrometer, the temperature interval (1400–1700 K) was divided into two ranges. This yielded a total of eight experiments on four tubular specimens. The desired heating rate in a given temperature range was achieved by adjusting a resistance in series with the specimen prior to each experiment. The heating rates in experiments on tubular specimens ranged typically from 1800 to 2100 $K \cdot s^{-1}$, corresponding to current pulses of 650 to 600 ms in duration. In experiments on strip specimens, the heating rates ranged typically from about 500 to 7000 $K \cdot s^{-1}$, corresponding to current pulses of 1500 to 250 ms in duration.

Upon completion of the experiments, the high-speed pyrometer was calibrated by means of a tungsten filament reference lamp which, in turn, had been calibrated against the NBS Photoelectric Pyrometer by the Radiometric Physics Division at NBS. All temperatures reported in this work are based on the International Practical Temperature Scale of 1968 [5].

3. RESULTS

In all computations, the geometrical quantities were based on their room temperature (295 K) dimensions. The results on specific heat capacity and electrical resistivity obtained from individual experiments are given in Tables A1 and A2 of the Appendix. The final values for the properties given at 50-K temperature intervals in Table II were computed by fitting (least squares approximation) the results presented in the Appendix to polynomials in temperature.

Table II. Smoothed Specific Heat Capacity and Electrical Resistivity of Low Carbon 304 Stainless Steel

T (K)	c_p(J · kg^{-1} · K^{-1})	ρ ($\mu\Omega$ · cm)
1400	675.2	122.5
1450	679.9	123.5
1500	686.2	124.4
1550	693.8	125.3
1600	702.9	126.2
1650	713.4	126.9
1700	725.4	127.7

3.1. Specific Heat Capacity

Specific heat capacity was computed from data taken during the heating period. The radiative heat loss was, in all cases, less than 2% at 1400 K and approximately 3% at 1700 K of the input power. A correction for this loss was made based on the hemispherical total emittance results obtained during the same experiments. The function for specific heat capacity (SD = 0.5%) that represents the results in the temperature range 1400–1700 K is

$$c_p = 1127 - 7.265 \times 10^{-1}\, T + 2.884 \times 10^{-4}\, T^2 \tag{1}$$

where T is in K and c_p is in J · kg^{-1} · K^{-1}.

3.2. Electrical Resistivity

The electrical resistivity was determined from the same experiments that were used to calculate specific heat capacity. The function for electrical resistivity (SD = 0.2%) that represents the results in the temperature range 1400–1700 K is

$$\rho = 75.59 + 4.695 \times 10^{-2}\, T - 9.592 \times 10^{-6}\, T^2 \tag{2}$$

where T is in K and ρ is in $\mu\Omega$ · cm. In the computation of electrical resistivity, the cross-sectional area was obtained from a measurement of specimen weight and from the value of density (7.885 g · cm^{-3}) determined by measurements on a cylindrical sample of specimen material. The measurements, before the pulse experiments, of the electrical resistivity of the four tubular specimens at 290 K with a Kelvin bridge yielded an average value of 72.8 $\mu\Omega$ · cm with an average absolute deviation of 0.3% and a maximum absolute deviation of 0.6%.

3.3. Hemispherical Total Emittance

Hemispherical total emittance was computed from data taken during both heating and initial free radiative cooling periods. The results of measurements in the temperature range 1500–1600 K did not show any definitive variation of emittance with changing temperature. A value of 0.37 was obtained by averaging all the results (average absolute deviation $\simeq 2\%$; maximum absolute deviation $\simeq 4\%$).

3.4. Melting Point

The temperature of the tubular specimens was measured before and during the initial melting period until the specimen collapsed. An abrupt decrease in the rate of temperature rise (to about 10% of the premelting heating rate) indicated the transition through the solidus point. Typical results for the specimen during the onset of melting are shown in Fig. 1. The melting point (solidus point) for each specimen was obtained from the intersection, along the temperature vs time function, of a linear fit to the melting "plateau" and a quadratic fit to the temperatures before melting determined by the least-squares method. The results are presented in Table III. The average melting point of the four specimens is 1706.6 K, with an average absolute deviation from the mean of 0.7 K and a maximum absolute deviation of 1.4 K. It may be concluded that the melting point of the low carbon 304 stainless steel studied in this work is 1707 K.

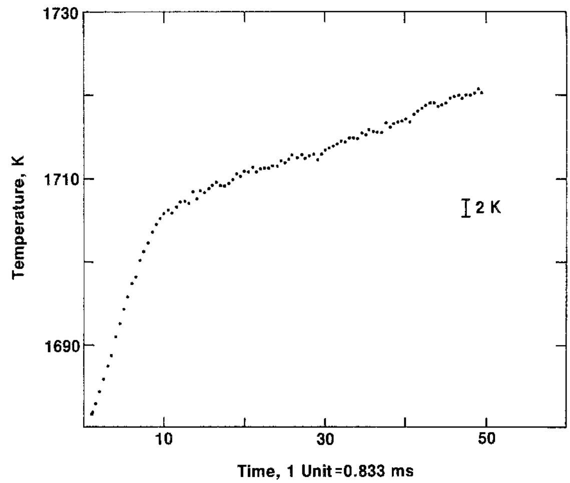

Fig. 1. Variation of the temperature of AISI type 304L stainless steel (specimen 3) as a function of time near and at its melting point.

Table III. Summary of Measurements of the Melting Point of Low Carbon 304 Stainless Steel

	Premelting period		Melting period			
Specimen number	Heating rate[a] ($K \cdot s^{-1}$)	Standard deviation[b] (K)	Number of temperatures[c]	Slope of plateau[d] ($K \cdot s^{-1}$)	Melting point[e] (K)	Standard deviation[f] (K)
1	1970	0.5	70	203	1708.0	0.3
2	1960	0.4	72	217	1706.6	0.4
3	1970	0.5	71	210	1706.2	0.4
4	1930	0.5	78	208	1705.7	0.5

[a]Derivative of the temperature vs time function (at approximately 10 K below the melting point) obtained by fitting the temperature data before melting to a quadratic function in time with the least squares method.

[b]Standard deviation of an individual temperature from the least-squares fit to the temperatures before melting.

[c]Number of temperatures used in obtaining a linear temperature vs time function during the melting period.

[d]Derivative of the temperature vs time function obtained by fitting the temperature data during the melting period to a linear function of time by the least-squares method.

[e]Corresponds to the intersecton, along the temperature vs time function, of a linear fit to the melting plateau and a quadratic fit to the temperatures before melting by the least-squares method.

[f]Standard deviation of an individual temperature from the smooth temperature vs time function (linear) obtained by the least-squares method.

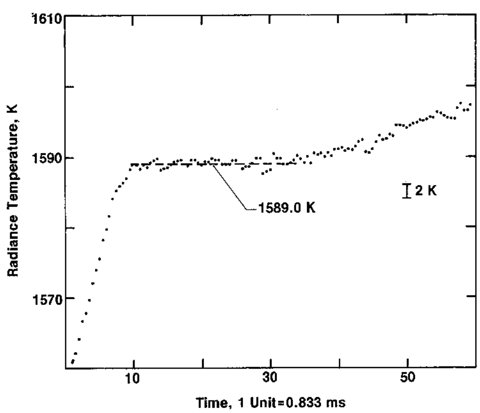

Fig. 2. Variation of the radiance temperature (at 653 nm) of AISI type 304L stainless steel (specimen 1) as a function of time near and at its melting point.

3.5. Radiance Temperature at the Melting Point

Radiance temperature measurements were performed on the strip specimens at 653 nm, which corresponds to the effective wavelength of the pyrometer's interference filter. The bandwidth of the filter was 10 nm. The circular area viewed by the pyrometer was 0.2 mm in diameter. Typical results are given in Fig. 2 for the variation of the specimen radiance temperature during melting, which manifested itself by an arrest in the temperature rise, forming a plateau during the initial melting period; this was followed by a further rise in temperature at approximately 10% of the premelting heating rate until the specimen collapsed. A single value for the

Table IV. Summary of Measurements of the Radiance Temperature (at 653 nm) of Low Carbon 304 Stainless Steel During Melting

	Premelting period		Initial melting period				
Specimen number	Heating rate[a] ($K \cdot s^{-1}$)	Standard deviation[b] (K)	Number of temperatures[c]	Slope at plateau[d] ($K \cdot s^{-1}$)	Plateau temp. difference[e] (K)	Radiance temp. at melting pt.[f] (K)	Standard deviation[g] (K)
1	2220	0.4	48	5.0	0.2	1589.0	0.6
2	850	0.5	84	13.0	0.9	1588.2	0.6
3	3840	0.6	30	10.2	0.3	1590.4	0.6
4	6300	0.7	12	−92.0	−0.9	1590.0	0.7
5	7000	0.6	14	3.9	0.1	1589.7	0.5
6	2470	0.5	44	7.6	0.3	1589.7	0.6
7	470	0.7	174	23.1	3.3	1589.4	1.2
8	570	0.8	114	21.0	2.0	1589.2	0.8
9	580	0.7	129	22.2	2.4	1589.3	0.9
10	2540	0.7	30	47.1	1.2	1589.5	0.7
11	4900	0.9	23	20.8	0.4	1590.5	1.0
12	4500	0.7	25	34.7	0.7	1589.4	0.8

[a]Derivative of the temperature vs time function (at approximately 10 K below the melting plateau) obtained by fitting the temperature data before melting to a linear function in time with the least-squares method.

[b]Standard deviation of an individual temperature from the least-squares fit to the temperatures before melting.

[c]Number of temperatures used in averaging the results at the plateau to obtain an average value for the radiance temperature at the melting point of the specimen.

[d]Derivative of the temperature vs time function obtained by fitting the temperature data at the plateau to a linear function in time by the least-squares method.

[e]Maximum radiance temperature difference between the beginning and the end of the plateau based on the linear temperature vs time function.

[f]The average (for a specimen) of measured radiance temperatures at the plateau.

[g]Standard deviation of an individual temperature as computed from the difference between the measured value and the average plateau radiance temperature.

radiance temperature at the melting point was obtained by averaging the temperatures at the plateau. The results are presented in Table IV for heating rates in the range 500–7000 K · s^{-1}. The average radiance temperature at the melting point for the specimens is 1589.5 K, with an average absolute deviation of 0.4 K and a maximum absolute deviation of 1.3 K. It may be concluded that the radiance temperature at the melting point of low carbon 304 stainless steel is 1590 K.

3.6. Normal Spectral Emittance

The normal spectral emittance at the melting point was determined from the results of the radiance temperature (obtained from measurements on strip-shaped specimens) and the melting point (obtained from measurements on tubular specimens). Computations, based on Planck's law, yielded a value of 0.385 for the normal spectral emittance (at 653 nm) at the melting point of the stainless steel.

3.7. Estimate of Errors

The details of estimating errors in measured and computed quantities using the present measurement system are given in an earlier publication [4]. In the present work, the specific items were recomputed whenever the conditions differed from those in the earlier publication. The results are summarized in Table V.

4. DISCUSSION

Considering the wealth of literature data on stainless steels, there is remarkably little information on the thermophysical properties of AISI type 304L at temperatures above 1400 K. In Figs. 3 and 4 the smoothed values for

Table V. Summary of the Estimate of Errors

Quantity	Imprecision[a]	Inaccuracy[b]
Specific heat capacity	0.5%	3%
Electrical resistivity	0.2%	2%
Hemispherical total emittance	2%	5%
Melting point	1 K	8 K
Radiance temperature (at melting point)	1 K	8 K
Normal spectral emittance (at melting point)		3%

[a]Imprecision refers to the standard deviation of a quantity as computed from the difference between the measured value and that from the smooth function obtained by the least-squares method.

[b]Inaccuracy refers to the estimated total error (random and systematic).

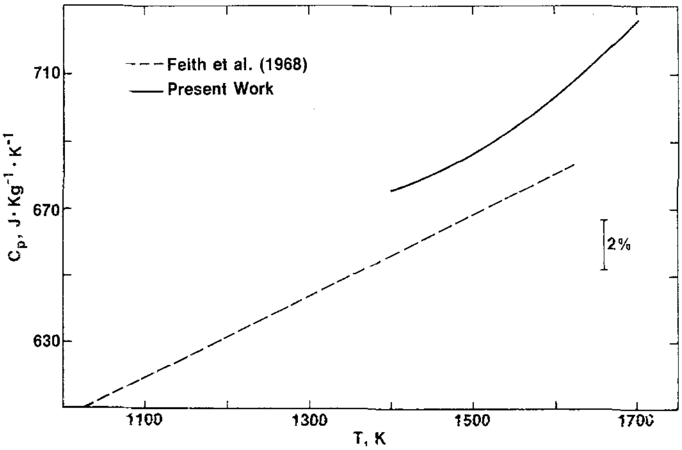

Fig. 3. Specific heat capacity of AISI type 304L stainless steel reported in the literature.

specific heat capacity and electrical resistivity listed in Table II are compared with the results of Feith et al. [6], which appear to be the only literature data available near the temperature range of the present work. Their results for specific heat capacity (derived from enthalpy measurements in the range 500–1600 K) are linear in temperature and are about 2% lower than our results in the temperature range common to both investigations. From Fig. 4,

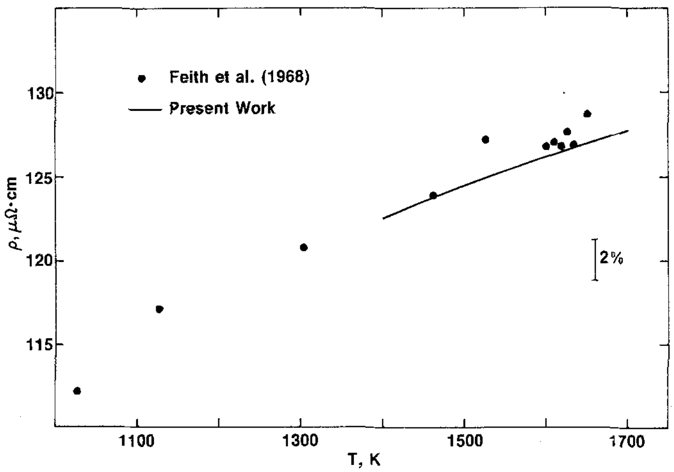

Fig. 4. Electrical resistivity of AISI type 304L stainless steel reported in the literature. The values of electrical resistivity are based on the room temperature dimensions of the specimens.

it can be seen that the electrical resistivity results of Feith et al. are about 1% higher than the results of the present work.

No data have been found in the literature on hemispherical total emittance of 304 stainless steel that correspond to the specimen conditions and the temperature range of the present measurements. The value of the hemispherical total emittance for a somewhat similar alloy (AISI type 310 stainless steel) at the highest reported temperature (about 1400 K) in the literature [7] is 0.29. This low value, compared to 0.37 (the value obtained in the present work for 1500–1600 K), may be attributed, in part, to the higher chromium-nickel content of 310 stainless steel: nominally 25% Cr–21% Ni, compared to about 18% Cr–9% Ni for the specimen material in our experiments.

In the present experiments related to melting, it was not possible to follow the entire melting process because of the hydrodynamic collapse of the specimens prior to reaching their liquid phase. Our work on tubular specimens yielded a value of 1707 K (at a heating rate of about 2000 K $\cdot$ s^{-1}) for the solidus point (or melting point) of 304 stainless steel, which is somewhat higher than that implied by the melting range 1670–1727 K commonly cited in the reference literature (for example, see *Metals Handbook* [8]).

In an effort to check for evidence of superheating in melting, we carried out a series of melting experiments on strip specimens at heating rates in the range 500 to 7000 K $\cdot$ s^{-1}. The results of the individual experiments are presented in Fig. 5, where the deviations from the average radiance temperature at the melting point (1589.5 K) are plotted as a function of the heating

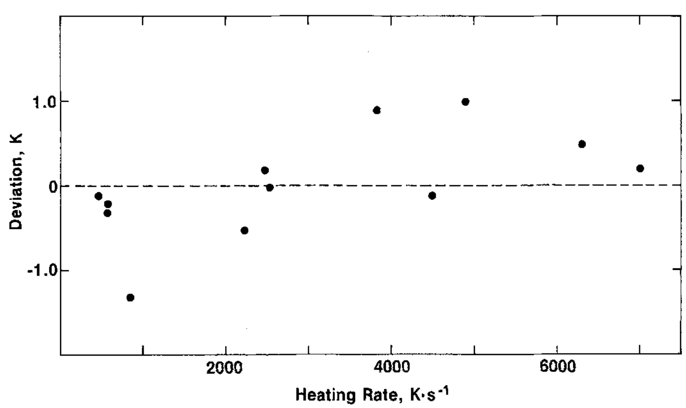

Fig. 5. Deviations from the average radiance temperature (1589.5 K) at the melting point as a function of the heating rate used in the individual experiments.

rate. It may be seen that, in the range of heating rates used, the variation in the results lie within the experimental imprecision (± 1 K), and thus do not indicate any effect of heating rate on the melting point.

We have seen in Figs. 1 and 2 that, as 304L stainless steel begins to melt, its true temperature increases at a rate that is about 10% of the premelting heating rate, whereas its surface radiance temperature remains approximately constant during the initial melting phase and then increases at about 10% of the premelting rate. This suggests that, during the initial melting period, the normal spectral emissivity decreases by about 3%.

Measurements of the normal spectral emittance at 665 nm on several stainless steel alloys (not including type 304L) under different conditions were reported in the literature [9] for temperatures in the range 1100–1500 K. There is considerable scatter in the values of normal spectral emittance for the different alloys at 1500 K, ranging between 0.3 and 0.4. The value of 0.385 obtained at the melting point (1707 K) of 304L stainless steel in the present work is consistent with these literature values.

ACKNOWLEDGMENTS

This work was supported in part by the U.S. Department of Energy through the Argonne National Laboratory. The encouragement and interest shown by L. Leibowitz of the above Laboratory throughout the course of this work is greatly appreciated. The authors also express their gratitude to M. S. Morse for his help with the electronic instrumentation.

APPENDIX: TABLES A1 AND A2

(See pages that follow.)

Table A1. Experimental Results for the Specific Heat Capacity of Low Carbon 304 Stainless Steel

	Specimen 1		Specimen 2		Specimen 3		Specimen 4	
T (K)	c_p ($J \cdot kg^{-1} \cdot K^{-1}$)	Δc_p[a] (%)	c_p ($J \cdot kg^{-1} \cdot K^{-1}$)	Δc_p[a] (%)	c_p ($J \cdot kg^{-1} \cdot K^{-1}$)	Δc_p[a] (%)	c_p ($J \cdot kg^{-1} \cdot K^{-1}$)	Δc_p[a] (%)
Range I								
1400	667.0	−1.3	682.2	+1.0	676.4	+0.1	673.5	−0.3
1450	674.8	−0.8	685.7	+0.8	681.9	+0.2	682.5	+0.3
1500	682.3	−0.6	688.8	+0.3	686.9	+0.1	691.4	+0.7
1550	689.4	−0.7	691.4	−0.4	691.6	−0.4	700.4	+0.9
Range II								
1550	691.4	−0.4	692.0	−0.3	693.4	−0.1	694.5	+0.1
1600	702.8	−0.1	702.6	−0.1	704.5	+0.2	704.4	+0.2
1650	714.4	+0.1	713.3	−0.1	715.8	+0.3	714.2	+0.1
1700	726.4	+0.1	724.1	−0.2	727.4	+0.2	723.9	−0.2

[a] Δc_p is the percentage deviation of the individual results from the smooth function defined by Eq. (1).

Table A2. Experimental Results for the Electrical Resistivity of Low Carbon 304 Stainless Steel

	Specimen 1		Specimen 2		Specimen 3		Specimen 4	
T (K)	ρ ($\mu\Omega \cdot$ cm)	$\Delta\rho^a$ (%)	ρ ($\mu\Omega \cdot$ cm)	$\Delta\rho^a$ (%)	ρ ($\mu\Omega \cdot$ cm)	$\Delta\rho^a$ (%)	ρ ($\mu\Omega \cdot$ cm)	$\Delta\rho^a$ (%)
Range I								
1400	122.9	+0.3	122.5	−0.1	122.4	−0.1	122.2	−0.3
1450	123.9	+0.3	123.6	+0.1	123.4	−0.1	123.2	−0.2
1500	124.9	+0.4	124.5	+0.1	124.4	−0.1	124.1	−0.3
1550	125.7	+0.3	125.4	+0.1	125.3	−0.1	125.0	−0.3
Range II								
1550	125.7	+0.3	125.4	+0.1	125.1	−0.2	124.9	−0.3
1600	126.6	+0.3	126.2	+0.1	126.0	−0.1	125.7	−0.4
1650	127.4	+0.4	127.0	+0.1	126.8	−0.1	126.6	−0.3
1700	128.2	+0.4	127.8	+0.1	127.5	−0.1	127.3	−0.3

[a] $\Delta\rho$ is the percentage deviation of the individual results from the smooth function defined by Eq. (2).

REFERENCES

1. A. Cezairliyan, *High Temp.-High Press.*, **11:** 9–27 (1979).
2. G. M. Foley, *Rev. Sci. Instrum.* **41:** 827–834 (1970).
3. A. Cezairliyan, *J. Res. Natl. Bur. Stand.* **75C:** 7–18 (1971).
4. A. Cezairliyan, M. S. Morse, H. A. Berman, and C. W. Beckett, *J. Res. Natl. Bur. Stand.* **74A:** 65–92 (1970).
5. International Committee for Weights and Measures, "The International Practical Temperature Scale of 1968," *Metrologia* **5:** 35–44 (1969).
6. A. D. Feith, R. A. Hein, C. P. Johnstone, and P. N. Flagella, in *Thermal Conductivity, Proceedings of the Eighth Conference* (1968), C. Y. Ho and R. E. Taylor, eds. (Plenum, New York, 1968), pp. 1051–1065.
7. Pratt and Whitney Aircraft, PWA-2309, NASA-CR-58054 (1964), 1–83.
8. *Metals Handbook,* 8th edn., Vol I. (Am. Soc. Metals, 1961).
9. Y. S. Touloukian and D. P. DeWitt, *Thermal Radiative Properties, Thermophysical Properties of Matter,* Vol. 7 (IFI/Plenum, New York, 1979).